6 Nuclear mass, nuclear size and nuclear matter

The nucleus was identified in the α-particle scattering experiments of Rutherford and Geiger because of the concentration of the positive charge Ze of the nuclear protons and of nearly the whole mass of the atom within a volume of radial extent less than about 10^{-14} m. Following the recognition of the fundamental neutron–proton structure of the nucleus, interest in the charge as an observable property now centres on its radial and angular distribution, on the interpretation of this distribution in terms of model wavefunctions, and on the effects of the electromagnetic interaction on nuclear structure. A complete theory of the charge density must also allow for the part played by exchanged particles such as pions and for the formation of nucleon isobars. The nuclear mass is a more fundamental property in the sense that it embodies not only the baryon number $B = N + Z = A$ but also energies derived from the basic nucleon–nucleon interaction, modified, if need be, by the inclusion of many-body interactions which cannot be sensed by the two-body scattering experiments described in Chapter 5. Because of the strong interaction between nucleons, the spatial distributions of charge and mass must be similar.

The calculation of the properties of finite nuclei from an assumed internucleon potential is an undertaking of considerable technical difficulty. It is useful, however, as an intermediate step to consider the nature of an infinite nuclear medium to see whether any general trends in nuclear mass values can be predicted. An immediate result of such a consideration is an understanding of the reasons why many nuclear properties, as well as mass, show the persistence of single-particle motion in a many-body system. The resulting *shell structure* is considered later (Ch. 7); the present chapter is primarily concerned with bulk properties.

6.1 The mass tables; binding energy

Two scales for mass measurements are now recognized:

(*a*) *The absolute scale*, related to the kilogram.

(*b*) *The atomic mass scale*, defined by setting the mass of one atom of the nuclide ^{12}C equal to 12·000 . . . atomic mass units (a.m.u. or u).

The absolute value of the atomic mass unit is obtained by noting that for 1 mole of ^{12}C (0·012 kg):

$$0{\cdot}012\,\text{kg} = N_A \times 12\,\text{a.m.u.}$$

where N_A is Avogadro's number, i.e. the number of atoms in one mole on the physical scale. This gives

$$1\,\text{a.m.u.} = 0{\cdot}001/N_A\,\text{kg} = 1{\cdot}661 \times 10^{-27}\,\text{kg} = 931{\cdot}481\,\text{MeV}/c^2$$

Both N_A and the a.m.u. depend on the standard substance, and were slightly different when masses were referred to ^{16}O.

Any particle mass may be specified in any of these units. Usually for general calculations kilograms are used, for particle physics kinematics, MeV/c^2, and for nuclear structure studies, a.m.u. Mass tables, such as those of Reference 6.1, give the masses of *neutral atoms* in a.m.u. rather than those of bare nuclei since the former are obtained as relative values directly by mass spectrometry. The atomic mass $M(A, Z)$ of a nuclide, i.e. a specific nucleus of mass number A, is related to the *nuclear mass* M_N by the equation

$$M(A, Z) = M_N + Zm_e - B(Z)/c^2 \qquad (6.1)$$

where m_e is the mass of the electron and $B(Z)$ the total electron binding energy. The binding energy term can be estimated from known X-ray energies not to exceed about 10^{-3} per cent of the atomic mass $M(A, Z)$ even for the heaviest elements and it may usually be neglected. The expression 'nuclear mass' is often loosely used to mean the neutral-atom mass in a.m.u.

The relative masses of all stable isotopes have now been determined with a precision of the order of 1 part in 10^6 by the refined techniques of mass spectrometry. Similar techniques, based on the deflection of charged particles in electric and magnetic fields, are used in the most precise determinations of nuclear reaction energy releases, which are related to mass changes through the equation

$$\Delta E = c^2\,\Delta M \qquad (6.2)$$

in which, of course, only changes of binding energy and not changes of the mass of the nucleons are involved. Combination of the data obtained in these ways leads to the present mass tables (Ref. 6.1), of which a small section is given in Table 6.1; the accuracy claimed in the relative atomic masses is better than 1 part in 10^6 for masses of the order of 30 a.m.u., corresponding with a determination of reaction energy released to a precision of a few keV or better.

TABLE 6.1 Atomic mass table (Ref. 6.1)

Nuclide $^{A}_{Z}$	*Atomic mass* a.m.u.	$B(A, Z)$ MeV	B/A MeV/*nucleon*	$S_n(A, Z)$ MeV	$P_n(A, Z)$ MeV
$^{131}_{54}$Xe	130·905 08 ± 0·3*	1103·55	8·41	6·6	—
$^{132}_{54}$Xe	131·904 16 ± 0·3	1112·49	8·42	8·9	1·2
$^{133}_{54}$Xe	132·905 89 ± 0·9	1118·94	8·41	6·5	1·1
$^{134}_{54}$Xe	133·905 39 ± 0·5	1127·48	8·41	8·5	1·0
$^{135}_{54}$Xe	134·907 14 ± 1·2	1133·93	8·40	6·45	0·9
$^{136}_{54}$Xe	135·907 22 ± 0·6	1141·92	8·40	8·0	1·4
$^{137}_{54}$Xe	136·911 75 ± 2·2	1145·78	8·36	3·9	—

* The errors in the mass values (a.m.u.) refer to the last significant figure.

The mass tables show that nuclidic masses are sufficiently near to multiples of the hydrogen-atom mass to suggest that nuclei are built up of particles of mass comparable with that of the proton, and this is consistent with a neutron–proton model. If this model is assumed the *total binding energy* $B(A, Z)$ of the nucleus (A, Z), which is the work required to break down the nucleus into Z protons and N $(= A - Z)$ neutrons, is given by the equation

$$B(A, Z) = ZM_H + NM_n - M(A, Z) \tag{6.3}$$

This expresses $B(A, Z)$ in a.m.u., but conversion to MeV is straightforward; typical values are given in Table 6.1 together with the average binding energy per nucleon B/A. The definition (6.3) implies that a stable nucleus has a positive binding energy, though a *negative* total energy with respect to that of its uncombined constituents at infinite separation.

The *separation energy* $S(A, Z)$ of a *specific particle*, e.g. a neutron, in the nucleus (A, Z) is the work required to remove that particle from the nucleus. For a neutron this converts the nucleus (A, Z) to the nucleus $(A - 1, Z)$ so that, for the least-bound particle,

$$\begin{aligned} S_n(A, Z) &= B(A, Z) - B(A - 1, Z) \\ &= M(A - 1, Z) - M(A, Z) + M_n \end{aligned} \tag{6.4a}$$

The S_n values calculated from this expression are greater for even N than for odd N (cf. Fig. 7.2) and a similar staggering effect is seen in the proton separation energies. This is due to attractive forces between identical pairs of nucleons with opposite spins in similar states of motion. If the average trend of separation energies is required, an alternative definition

$$S_n(A, Z) = \tfrac{1}{2}[B(A + 1, Z) - B(A - 1, Z)] \tag{6.4b}$$

may be used. To exhibit the pairing effect, however, it is useful to

define a *pairing energy* P by the expression

$$P_n(A, Z) = (-1)^N \tfrac{1}{4}\{2S_n(A, Z) - S_n(A-1, Z) - S_n(A+1, Z)\} \tag{6.5}$$

for neutron pairing and similarly an energy $P_p(A, Z)$ for proton pairing. Values of P_n derived from S_n-values given by equation (6.4a) are shown in Table 6.1.

Separation energies are often determined from the Q-values for transfer or capture reactions (see Ex. 6.4).

6.2 Nuclear size

If a nucleus is held together by short-range forces it is expected to have a constant density (liquid-drop model). If also it is spherical, with a sharp edge, then the radius R for mass number A is easily seen to be

$$R = r_0 A^{1/3} \tag{6.6a}$$

For such an idealized, uniform object the potential energy of a hypothetical strongly-interacting positive charge $Z_1 e$ as a function of distance from the nuclear centre would be approximately as shown in Fig. 6.1, in which the Coulomb repulsion is artifically

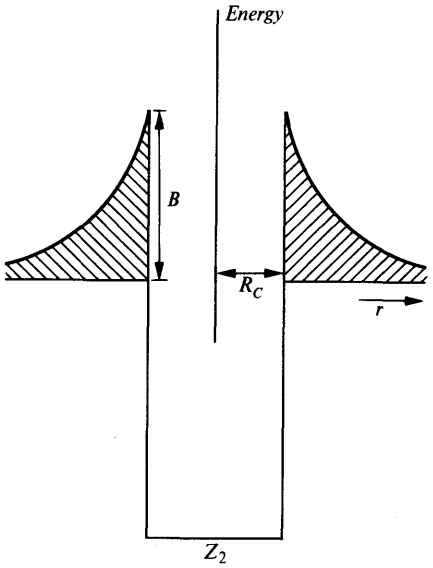

Fig. 6.1 Idealized potential well of radius R_C with barrier of height B. Spherical symmetry is assumed.

terminated at a radius R_C where it creates a *barrier* of height B given by

$$B = Z_1 Z_2 e^2 / 4\pi\varepsilon_0 R_C \tag{6.6b}$$

if the nuclear charge is $Z_2 e$. For $Z_1 = 1$, $Z_2 = 92$ and $R_C = 7$ fm, $B = 19$ MeV. At smaller distances the Coulomb potential is replaced by the attractive nuclear potential; for a hypothetical point-neutron there is simply a uniform well of radius R_C. In both cases centrifugal potentials are disregarded.

This uniform model is adequate, with a suitable choice of r_0 in equation (6.6a), for the calculation of the Coulomb term in the mass formula, equation (6.10), and for estimating penetrabilities and geometrical cross-sections (Ch. 11) but it is a highly inadequate representation of the density of nuclear matter within a nucleus. To make the concept of nuclear size more realistic we now consider exploration of the interaction region shown in Fig. 1.1 using (*a*) an electromagnetic probe, specifically high-energy electrons, and (*b*) a hadronic probe, specifically nucleons.

(i) *Electron scattering.* If the particle approaching the nucleus is an electron, there is no attractive nuclear force, but the Coulomb force itself becomes attractive. The scattering can reveal detail of the charge distribution if the reduced de Broglie wavelength of the incident electrons is less than a typical nuclear dimension, say $\lambda\!\!\!^{-} \approx 1$ fm, $E \approx 200$ MeV. The electron is not known to have any structure and, therefore, behaves like a point charge. The effect of finite size of the target is then seen directly as a reduction of the scattering at a given angle below that expected for relativistic point-charge scattering as calculated by Mott. In the pioneer experiments of Hofstadter and his collaborators at Stanford, using linear accelerators providing electrons with energy up to 550 MeV, the ratio of observed and calculated intensities at a given angle was expressed as the square of a form factor F. Since the electromagnetic interaction is completely known F can be given directly in terms of the nuclear charge density $\rho(r)$ on the assumption that the scattering can reasonably be described by the Born approximation of quantum mechanics. In terms of the momentum transfer $\boldsymbol{q}$ to the nucleus ($Z_2 = Z$) as defined, for instance, in equation (1.6)

$$F(q) = (4\pi\hbar/qZe) \int_0^\infty \rho(r) \sin(\boldsymbol{q} \cdot \boldsymbol{r}/\hbar) r \, \mathrm{d}r \tag{6.7a}$$

where $q = |\boldsymbol{q}| = (2E/c) \sin\theta/2$, E is the total energy of the electron and θ the angle of scattering, both in the c.m. system. To simplify this and similar formulae it is usual to write the momentum transfer as $\hbar\boldsymbol{q}$ so that q becomes a reciprocal length and (6.7a) reads

$$F(q) = (4\pi/qZe) \int_0^\infty \rho(r) \sin(\boldsymbol{q} \cdot \boldsymbol{r}) r \, \mathrm{d}r \tag{6.7b}$$

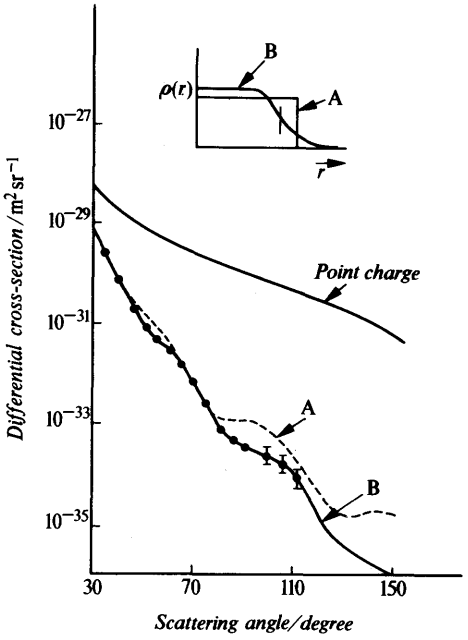

Fig. 6.2 Scattering of 153-MeV electrons by gold with (inset) charge distributions that may be used to fit the data points; the 'half-way' radius is marked. Reproduced from *Nuclear Structures* Vol. I, 1969, by Aage Bohr and Ben R. Mottleson with permission of the publishers, Addison-Wesley/W. A. Benjamin Inc.

Experimental data from which values of $F(q)$ may be derived are shown in Fig. 6.2. If a sufficiently large range of q-values can be covered then $\rho(r)$ can be obtained by making a Fourier transform of $F(q)$ with respect to q. In general, however, this is not possible and a density distribution must be assumed e.g.

$$\rho(r) = \rho_0/[1+\exp(r-R_{1/2})/a] \tag{6.8a}$$

Comparison with experiment then gives best-fit values for the half-way radius $R_{1/2}$ and the surface thickness parameter a. In the inset to Fig. 6.2 such a distribution is shown, together with the uniform distribution of radius R_C which best fits the data points. The mean-square radius for a given $\rho(r)$ is defined as

$$\langle r^2\rangle = (1/Ze)\int_0^\infty r^2\rho(r)4\pi r^2\,\mathrm{d}r \tag{6.8b}$$

and for the density distribution (6.8a) we have $\langle r^2\rangle^{1/2} < R_{1/2} < R_C$. For a wide range of nuclei with $A > 20$, an $A^{1/3}$ dependence of $R_{1/2}$ is found.

It should be noted that this very direct determination of charge density does not give precisely the distribution of nuclear protons

because the proton itself has a charge structure which must be folded in with the spatial density to give the observed $\rho(r)$. It should also be observed that the use of the q-dependence of elastic scattering in the present way is an example of a general method of *structure* determination that is used in other fields of physics. We shall encounter later (Sect. 9.4.3) a similar use of the q-dependence of *inelastic* form-factors but the information then obtained is mainly *spectroscopic.*

Other methods of determining the mean-square radius of the charge distribution, or its variation from one nucleus to another, are observations of:

(*a*) energy displacements in the spectra of muonic atoms (Sect. 3.3);
(*b*) the Coulomb energy of mirror nuclei such as ^{13}C, ^{13}N which have the same structure except that Z and N are interchanged;
(*c*) optical and X-ray isotope shifts (Sect. 8.1.2).

The results of all these methods are consistent with those of the electron-scattering determinations.

(ii) *Nucleon scattering.* The density distribution of nuclear matter $\rho_m(r)$, as distinct from that of nuclear protons $\rho_p(r)$, is best studied by proton–nucleus scattering at energies in excess of the Coulomb barrier. Such experiments are described in Section 7.2.4 in connection with the shell-model potential, and in Section 11.4 in connection with the optical model for nuclear reactions. Here, it will only be noted that despite the facts that the probe is not a point particle and that the interaction is not known, it is indeed possible to obtain potential parameters. The radial variation of the interaction potential is usually taken to have the form used for the charge density in equation (6.8a) with an overall negative sign but as it is not certain that the half-way radius means exactly the same thing we shall denote it by R_V. (It is, in principle, possible to predict R_V from $R_{1/2}$ (matter) by folding the nucleon–nucleon interaction with a density distribution.)

Experimental results confirm that R_V has the expected $A^{1/3}$ dependence and suggest that the radial dependence of the matter density is very similar to that of the charge density. Only for the heaviest nuclei is there some indication of an increased radius for the neutron distribution.

(iii) *Summary.* Inserting the best average values for r_0, nuclear size may be specified by the following radii for a spherical shape:

$$\begin{aligned} R_{1/2} &= 1{\cdot}1A^{1/3}\ \text{fm} && \text{(matter distribution)} \\ R_C &= (1{\cdot}2\text{–}1{\cdot}3)A^{1/3}\ \text{fm} && \text{(equivalent square well for charge distribution)} \\ R_V &= 1{\cdot}25A^{1/3}\ \text{fm} && \text{(optical potential)} \end{aligned} \qquad (6.9a)$$

Other radii, usually less well defined, will be used in this book,

especially in connection with heavy-ion collisions (Ch. 11). In such cases the crude picture of Fig. 6.1 is very far from the truth because nuclear interactions set in at an interparticle distance considerably greater than $1{\cdot}1(A_1^{1/3}+A_2^{1/3})$ fm. The *strong-absorption radius*, at which such processes are first seen, is approximately

$$R_{SA}=(1{\cdot}4\text{–}1{\cdot}5)(A_1^{1/3}+A_2^{1/3})\text{ fm} \qquad (6.9b)$$

6.3 The semi-empirical mass formula

This formula connects the experimental information on masses with predictions from the theory of nuclear matter. A simple spherical liquid drop of uniform density and radius given by equation (6.6a) is assumed, although independent particle motion is also invoked, as will be seen.

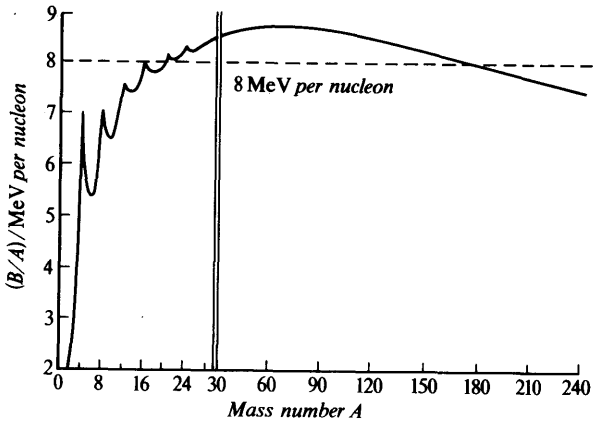

Fig. 6.3 Average binding energy per nucleon of the stable nuclei as a function of mass number (Ref. 2.1).

Figure 6.3 shows the dependence of the observed binding energy per nucleon B/A on the mass number A. The most important features of this diagram are:

(*a*) The appearance of approximately the same B/A (7·3 to 8·7 MeV) for all nuclei with $A>16$ so that for all but the lightest nuclei it is a good approximation to assume that B is proportional to A. If all pairs of nucleons in the nucleus interacted attractively, B would be more nearly proportional to A^2. It therefore follows that attractive interactions are, in effect, confined to near neighbours and that the total *volume energy* of the nucleus may be expressed in the form αA where α is a constant to be determined from the masses and to be predicted theoretically. A simple expression of this form,

however, overlooks the fact that nucleons near the surface of the nucleus will probably be less effective in producing binding than those in the interior. From equation (6.6a) the nuclear surface area varies as $A^{2/3}$ and the *surface energy* correction may be written $\beta A^{2/3}$.

(*b*) The general upward trend of B/A for the light nuclei. In a liquid-drop model, this trend is explained by the increasing ratio of the volume energy (αA) to the surface energy ($\beta A^{2/3}$) as A increases. There are marked increases of stability for $A = 4n$, $Z = N = 2n$ corresponding to equal numbers of neutrons and protons, which are not predicted by the liquid-drop model and must indicate a structure in which pairs of like particles can exist close together under attractive forces. If this effect is a general one there will be a correction when Z differs from N, since disregarding other effects the isobaric nucleus with $Z = N = A/2$ would be more stable. The resulting *asymmetry energy* may be estimated (see Ex. 6.1) from a model in which the nucleons fill the states of a Fermi distribution in accordance with the exclusion principle; it has the form $\gamma(A - 2Z)^2/A$ or $4\gamma T_z^2/A$ where T_z is the isobaric spin component (Sect. 5.6).

(*c*) The decrease of binding energy per nucleon from a maximum value of 8·7 MeV at $A = 60$, to 7·3 MeV at $A = 238$. This is due to the mutual electrostatic repulsion of the nuclear protons which does operate between all pairs because of the long-range nature of the force. In the liquid-drop model the corresponding *Coulomb energy* is simply the potential energy of a sphere of charge Ze whose radius is $\approx 1{\cdot}25A^{1/3}$ fm (Sect. 6.2); it is written $\varepsilon Z^2/A^{1/3}$ (sometimes $Z(Z-1)$ rather than Z^2).

In heavy nuclei the disruptive effect of the protons is compensated by the attractive bonds associated with an increased number of neutrons. The stability of such nuclei will be affected by the nature of the spatial states occupied by the nucleons and the importance of shell-structure corrections is now established (Sect. 11.7).

(*d*) The existence of the pairing energy $P(A, Z)$ given by equation (6.5). If the general trend of masses is that of the odd-A nuclei, then for the even-A nuclei those with Z, N even are more stable, and those with Z, N odd are less stable, than the average. This correction is additional to the asymmetry energy and is written $\delta(A, Z)$ where $\delta \approx P(A, Z)$ and explicitly (Ref. 6.2):

$\delta = 0$ for A odd

$\delta = +12A^{-1/2}$ MeV for A even, Z odd, sometimes given as $33{\cdot}5A^{-3/4}$ MeV

$\delta = -12A^{-1/2}$ MeV for A even, Z even, sometimes given as $-33{\cdot}5A^{-3/4}$ MeV

If now all these energies are expressed in the same units, e.g. a.m.u. or MeV, the mass of the neutral atom may be written

$$M(A, Z) = ZM_H + NM_n - \alpha A + \beta A^{2/3} + \gamma(A-2Z)^2/A + \varepsilon Z^2/A^{1/3} + \delta(A, Z) \quad (6.10)$$

where $\delta(A, Z)$ is negative for A even, Z even, zero for A odd, and positive for A even, Z odd. This is the *semi-empirical mass formula* giving the mass $M(A, Z)$ or the binding energy $B(A, Z)$ from equation (6.3) as a smoothly varying function of A and Z which may be fitted to the curve shown in Fig. 6.3. No corrections so far appear for shell structure.

Several sets of constants α, β, γ, ε have been proposed. With one set, due to A. E. S. Green, the values in MeV are $\alpha = 15{\cdot}8$, $\beta = 17{\cdot}8$, $\gamma = 23{\cdot}75$ and $\varepsilon = 0{\cdot}71$. The total binding energy of a nucleus of $Z = 100$, $A = 250$ would be

$$\begin{aligned} B &= ZM_H + NM_n - M(A, Z) \\ &= A[15{\cdot}8 - 2{\cdot}8 - 0{\cdot}95 - 4{\cdot}51 - \delta A^{b1}] \\ &= A[7{\cdot}5 - \delta A^{-1}]\,\text{MeV} \end{aligned}$$

showing that the corrections to the volume energy are substantial.

The use of the semi-empirical mass formula in indicating stability limits and in demonstrating the importance of shell structure will be mentioned in Sections 6.5 and 7.1.1. The next section will be devoted to a consideration of the origin of the volume energy term αA of the formula, since this must be a property of nuclear matter as well as of finite nuclei.

6.4 Nuclear matter

6.4.1 Characteristics

Nuclear matter is the result of an extrapolation of a typical heavy nucleus to a uniform infinite medium in which the numbers of neutrons and protons are equal, and no Coulomb forces exist. In such a system there is no preferred centre, and particle motions should be described by plane waves.

The physical properties of nuclear matter are summarized by stating the binding energy per particle E/A and the equilibrium density ρ, for which it is reasonable to assume that the binding energy reaches a maximum value. Numerical values of E/A are obtained by extrapolation from the semi-empirical mass formula (6.10) to the nuclear matter limit $A = \infty$, $N = Z$ which gives, with constants specified in Section 6.3,

$$E/A = (B/A)_\infty = \alpha = 15{\cdot}8\,\text{MeV} \quad (6.11)$$

The density ρ is found from electron-scattering determinations of the central charge-density of heavy nuclei and is usually taken to be

$$\rho = 3/4\pi r_0^3 = 0{\cdot}17 \text{ nucleons fm}^{-3} \tag{6.12}$$

using a radius parameter $r_0 = 1{\cdot}1$ fm.

Although nuclear forces are strong, they are insufficiently strong to confer the properties of a solid on nuclear matter, and this substance will be regarded as a degenerate Fermi gas containing two varieties of fermion. It is then possible to give an alternative expression for the density, exhibiting the maximum momentum $p_F = k_F\hbar$ belonging to such a system; k_F is the wavenumber. In terms of k_F

$$\rho = 2k_F^3/3\pi^2 \tag{6.13}$$

as in the electron theory of metals, remembering that for a given type of nucleon, the density is $\rho/2$. For nuclear matter, equations (6.12) and (6.13) give $k_F = 1{\cdot}38 \text{ fm}^{-1}$.

In such a Fermi gas the average kinetic energy of a particle is

$$\langle T \rangle = \tfrac{3}{5}(\hbar^2 k_F^2/2m_p) = 23 \text{ MeV} \tag{6.14}$$

for $k_F = 1{\cdot}38 \text{ fm}^{-1}$ so that with a volume energy term of 15·8 MeV the attractive field in nuclear matter must provide a binding energy of 38·8 MeV. It is the task of nuclear-matter theory to relate this binding energy to the properties of the internucleon force.

6.4.2 Theory of the binding energy

The first important fact about nuclear matter as a Fermi gas is that the Pauli exclusion principle prevents the close approach of like nucleons in the same state of motion, so that the effective interaction is less than would be expected for particles obeying classical statistics. The Pauli principle has the further effect that an interaction between two nucleons, which we regard as a scattering (Fig. 6.4*a*), is only possible if both nucleons after the interaction occupy vacant momentum states. Since all states are filled up to a momentum $p_F = \hbar k_F$, such a scattering process involves a high momentum transfer, and is suppressed, at least for particles well down in the Fermi sea. It is for this reason that single-particle motion can be envisaged in nuclear matter and in finite nuclei where it allows the persistence of shell-model orbital motion (Ch. 7). The scattering process shown in Fig. 6.4 is virtual and energy conservation must be restored by further processes that return the interacting particles to their original states.

The Pauli exclusion principle operates for like fermions whatever the form of interaction between them. Nucleons both like and

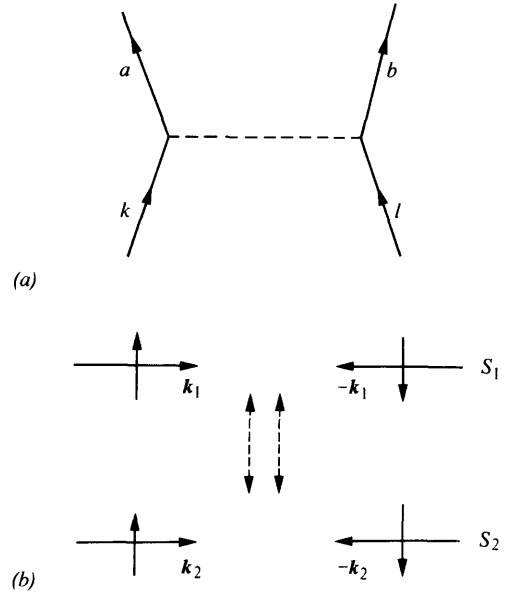

Fig. 6.4 (*a*) Particles k, l in the Fermi sea interact, leaving holes in the sea and becoming particles a, b above the sea. This is a virtual process contributing to the energy of nuclear matter. (*b*) Head-on collision of two nucleons with equal and opposite momenta and intrinsic spin.

unlike are also kept apart by the probable existence of a repulsive core of short range in their mutual interaction. This core may be very strong but the product of the core potential v and the actual wavefunction for two interacting particles ψ_{kl} will be finite if an interaction exists. We do not know what the actual wavefunction for the interacting pair is, but we may use a *model* wavefunction ϕ_{kl} and relate this to ψ_{kl} by the equation

$$G\phi_{kl} = v\psi_{kl} \tag{6.15}$$

where G is an *effective potential* which, with suitable choice of ϕ_{kl} may be less singular than the actual potential v. For nuclear matter the model wavefunctions ϕ_{kl} will be constructed from plane waves; for finite nuclei, oscillator functions are more appropriate.

The use of the effective potential in nuclear matter and nuclear model calculations is discussed in References 6.3 and 6.4. The key techniques in these calculations were developed by Brueckner, Bethe and Goldstone, who set up an operator equation for the effective potential G in the form

$$G\phi_k\phi_l = v\phi_k\phi_l + [vQ_{kl}/(e_{kl} - H_0)]G\phi_k\phi_l \tag{6.16}$$

where ϕ_k, ϕ_l are single-particle wavefunctions in a potential well U that represents the average field in nuclear matter, $H_0 = H_0(1) + H_0(2)$ is the unperturbed Hamiltonian operator, giving the energy of the two nucleons in the absence of correlations induced by their interaction, e_{kl} is the perturbed energy of the pair, and Q_{kl} is the Pauli factor that ensures that the particles occupy states permitted by the exclusion principle. If G is calculated from (6.16) generalized to a system of A particles, and used in the Schrödinger equation with any suitable H_0 and U, the energy of nuclear matter then involves the matrix elements of G between uncorrelated states, which are known, rather than the matrix elements of v between actual correlated states, which are unknown.

The details of these calculations will not be given here, since they are algebraically complex. It is found that the internucleon force introduces most perturbation in the s-waves, but even so the correlation disappears within a distance of about 2 fm. The tensor component of the effective internucleon force and the existence of exchange components in the central force jointly produce the nuclear matter saturation effect at the postulated equilibrium density. Typical results of matter calculations, for the so-called Reid soft-core potential, are given in Table 6.2, which shows the effect of introducing three-body and four-body effects. The uncertainties in some of the contributions to binding energy are such that the differences from the experimental value of 15·8 MeV is not unexpected. It may be concluded that the energy and density of nuclear matter are consistent with the properties of actual forces. It will also be noted from the table that the effective interaction in nuclear matter is density-dependent.

TABLE 6.2 Energy of nuclear matter (MeV) (from Ref. 6.4, p. 297)

k_F fm^{-1}	1·2	1·36	1·6
Two body	−27·71	−34·02	−42·05
Three body	−1·6	−1·59	−1·1
Four body	−0·9	−1·1	−1·5
Kinetic energy	17·92	22·97	31·85
E/A after corrections	−13·5	−14·1	−10·4

If nuclear matter with an unequal number of neutrons and protons is analysed in the same way, the coefficient of the asymmetry term in the semi-empirical mass formula may be found; it is also consistent with the experimental value (Sect. 6.3).

6.4.3 The pairing energy

On the assumption that the methods outlined in the previous section permit the definition of a short-range effective interaction in nuclear

matter, despite the existence of a repulsive core, one may further enquire whether any effects remain that may be attributed to the longer-range attractive parts of the internucleon force that are not included in the previous calculation. One such effect gives rise to the *pairing energy* $\delta(A, Z)$ that appears in the semi-empirical mass formula (6.10). This has little to do with the main distribution of nucleons in nuclear matter, but is of special significance in finite nuclei. It arises in a particular type of collision between like nucleons (Fig. 6.4*b*) in which the colliding pair has zero resultant linear momentum (in nuclear matter) or angular momentum (in a nucleus) and oppositely directed spins. The collision transfers the pair from a state S_1 with momentum vectors $\boldsymbol{k}_1$ to a state S_2 with momentum vectors $\boldsymbol{k}_2$, conserving momentum; further collisions return the pair to S_1, conserving energy. If the force between the particles is attractive, then it is found, as in the case of a superconducting metal, that a state containing such pairs is lowered in energy.

To see the origin of such an effect we consider for simplicity two like nucleons outside the Fermi sphere and we specify a small number of plane-wave two-particle states $S_1, S_2, \ldots, S_n$ which they may occupy. The two-particle wavefunctions, in the absence of interaction, will be written $\phi_1, \ldots, \phi_n$ and the *single*-particle kinetic energies will be taken as those corresponding with plane waves of momentum vector $\boldsymbol{k}$, i.e. $e_1 = \hbar^2 k_1^2/2m$, etc. The wavefunctions ϕ are solutions of the field-free Schrödinger equation

$$H_0\phi = E_0\phi \tag{6.17a}$$

and $E_0 = 2e_1$, etc. in this simple case.

When an interaction V exists, i.e. when collisions take place, the Schrödinger equation becomes

$$(H_0 + V)\psi = E\psi \tag{6.17b}$$

where the perturbed wavefunction ψ may be expanded in terms of the ϕ-functions in the form

$$\psi = \sum_{i=1}^{n} c_i\phi_i \tag{6.18}$$

The perturbed energies E are then obtained by substituting in (6.17b), multiplying through by a chosen ϕ_k^*, and taking an integral over all space using the orthogonality property of the ϕ's. This gives, using also equation (6.17a) for the unperturbed energies $2e_k$,

$$(2e_k - E)c_k + \sum_{1}^{n} c_i\langle\phi_k^*|\, V\,|\phi_i\rangle = 0 \tag{6.19}$$

where

$$\langle\phi_k^*|\, V\,|\phi_i\rangle = \int \phi_k^* V \phi_i \, \mathrm{d}^3\boldsymbol{r} \tag{6.20a}$$

We now assume that the interaction is confined to states with momenta very close to the Fermi momentum and that for all such states

$$\langle \phi_k^* | V | \phi_i \rangle = -F \tag{6.20b}$$

and is zero otherwise. We then have

$$c_k = CF/(2e_k - E) \tag{6.21}$$

where $C = \sum_1^n c_i$ and an eigenvalue equation is obtained in the form

$$1/F = \sum_1^n 1/(2e_k - E) \tag{6.22}$$

This may be solved graphically (Fig. 6.5) and gives the actual energies E in relation to the unperturbed energies $2e_k$. The figure shows that the lowest eigenvalue is shifted downwards more than the others, because of the form of equation (6.22), and if these latter states are close together the downward shift causes a gap in the sequence.

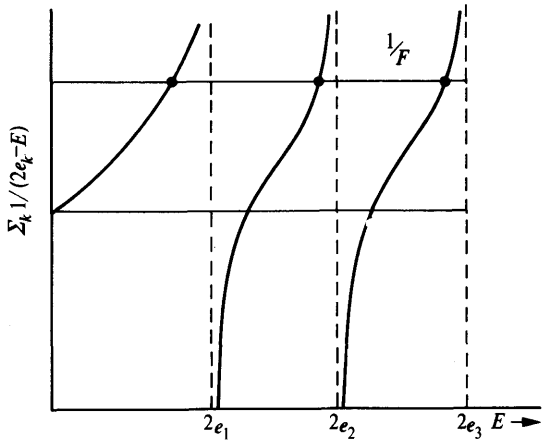

Fig. 6.5 Lowering of 'ground state' energy of two nucleons by the pairing interaction. The figure is a graphical solution of equation (6.22), in which the dotted lines represent unperturbed energy eigenvalues. The dots show the actual eigenvalues and indicate an increased displacement for the ground state (adapted from Ref. 6.4).

This treatment may be generalized and extended to the many-body problem with similar results. It is shown in Reference 6.4 that if V has the simple form of a delta-function interaction, the matrix element (6.20) indeed has a constant value and all pairs contribute in phase to a lowered energy.

In what follows we consider explicitly the case of finite nuclei, because the spectrum of basic states near the Fermi energy accentuates pairing effects in comparison with those same effects in

nuclear matter. The main consequences of pairing are that:

(*a*) The Fermi surface is no longer sharp and both holes below it and particles above it can co-exist. (Excitations that are mixtures of a particle state and a hole state are known as *quasiparticles.*)

(*b*) An *energy gap,* usually given as 2Δ, arises between the ground state and first excited state of many even–even nuclei (though not those that will be found in Ch. 7 to have closed major shells). Such gaps are known experimentally, and their appearance led A. Bohr, Mottelson and Pines originally to suggest that the ground state might exhibit superfluid properties. The difference between this state and other states with a similar constitution in terms of basic states is simply that there is a greater degree of coherence in the nuclear motion.

An odd–odd nucleus has two unpaired and dissimilar nucleons and its ground state may be expected to be displaced by an energy of the order of 2Δ above that of the isobaric even–even nucleus for this reason. From the semi-empirical mass formula, equation (6.10), we see that this difference is expressed by the quantity $2\delta(A, Z)$ so that δ is equal to half the energy gap. The pairing energy $P(A, Z)$ defined in equation (6.5) is then also approximately equal to Δ which is seen from Table 6.1 to be about 1 MeV at $A = 134$.

6.5 Nuclear stability

If nuclei are arranged in order of increasing N and Z on a rectangular grid, all nuclides of the same N (isotones) appear in, for example, horizontal lines and all nuclides of the same Z (isotopes) in vertical lines. This neutron–proton diagram, sometimes known as the Segrè chart, is shown for the naturally occurring nuclides in Fig. 2.1, p. 51. Stable nuclei of low mass number have $N = Z = A/2$ but medium-weight and heavy nuclei have many excess neutrons. The unstable nuclides mainly form a fringe to the band of stability but, for some elements, intermingle with the stable isotopes.

The semi-empirical mass formula is, of course, constructed to ensure that the stability of known nuclei is correctly predicted. For odd-A nuclei for instance, for which δ is zero, the most stable nucleus is that with an atomic number Z given by the setting $\partial/\partial Z[M(A, Z)] = 0$. From equation (6.10), remembering that $N = A - Z$, and using the constants due to Green

$$Z = A/(1{\cdot}98 + 0{\cdot}015A^{2/3}) \tag{6.23}$$

which shows that Z falls short of $A/2$ as A increases. Physically, this is due to the fact that Coulomb repulsion is a long-range force and that it becomes increasingly important with respect to short-range

nuclear forces as the nuclear charge increases. The repulsive effect has to be balanced by the presence of extra neutrons. These provide extra volume energy, but they must also conform with the Pauli principle and the extra kinetic energy (a disruptive effect) is represented by the asymmetry term. If, in fact, the variation of $B(A, Z)$ with A for constant Z, i.e. the dependence of B on neutron number is examined, equation (6.10) shows that $[\partial B/\partial A]_Z$ vanishes for $Z/A \approx \frac{1}{3}$, i.e. when there are twice as many neutrons as protons, additional neutrons do not contribute extra binding. If, however, the nucleus becomes very large indeed, so that gravitational forces can play a part, stability will again result in a body consisting mainly of neutrons; this is a *neutron star.*

If a third coordinate representing the atomic mass $M(A, Z)$ is added to the neutron–proton diagram, a three-dimensional *mass surface* is defined. Stable nuclei group round the bottom of a valley in this surface. Intersections of the mass surface by planes of constant A pick out groups of isobars comprising both stable and unstable nuclei. Formula (6.10) shows that for A constant, $M(A, Z)$ is a parabolic function of Z (Fig. 6.6). For odd A, one parabola is obtained but for even A there are two, separated by an energy $2\delta(A, Z)$.

From Fig. 6.6 there is just one stable isobar for A odd but for even A there may be two or three stable species. Stability is reached in an isobaric sequence by electron (β^-) or positron (β^+) emission or

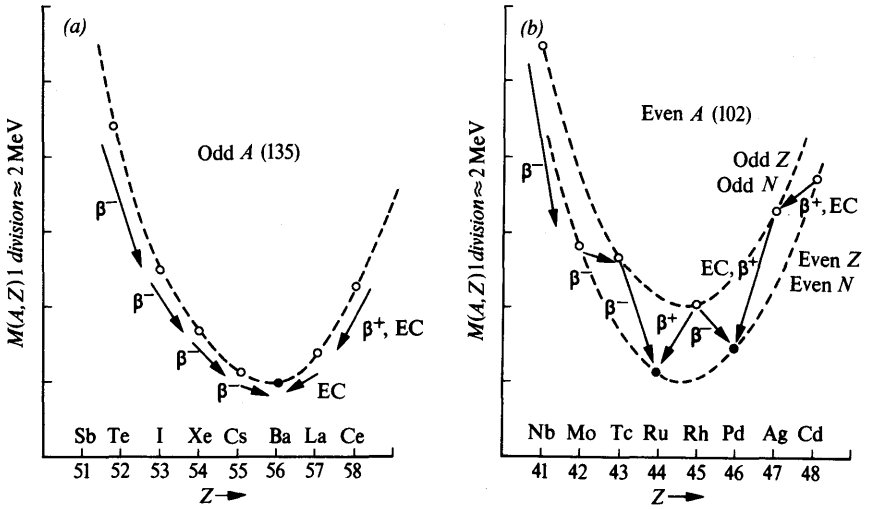

Fig. 6.6 Stability of isobars, showing atomic mass M plotted against atomic number Z. (*a*) Odd A. (*b*) Even A. Electron capture (EC) is in principle also possible whenever β^+-emission may take place (Ref. 2.1).

electron capture (EC) as indicated in the figure. Such radioactive decay processes are possible for a nuclide of atomic mass $M(A, Z)$ if this quantity is related to the mass $M(A, Z \pm 1)$ of the product nuclide by the following inequalities:

For electron decay to $M(A, Z+1)$	$M(A, Z) > M(A, Z+1)$
For positron decay to $M(A, Z-1)$	$M(A, Z) > M(A, Z-1) + 2m_e$ where m_e is the electron mass in a.m.u.
For atomic electron capture to $M(A, Z-1)$	$M(A, Z) > M(A, Z-1) + B_e$ where B_e is the ionization energy (in a.m.u.) for the electron captured in the neutral atom of charge $Z-1$.

(6.24)

These relations assume that the mass of the neutrino that is known to be emitted in such semi-leptonic processes (Sect. 2.1.6) is zero. If $\Delta M = [M(A, Z) - M(A, Z \pm 1)]\,\text{MeV/c}^2$ then the Q-values in MeV for the processes (6.24), defined in accordance with equations (1.7) and (1.20) as the kinetic energy available for all product particles (or quanta), are:

$$
\begin{aligned}
Q_{\beta^-} &= \Delta M \\
Q_{\beta^+} &= \Delta M - 2m_e c^2 \quad \text{(because the change of } Z \text{ frees an atomic electron in addition to the decay positron)} \\
Q_{EC} &= \Delta M - B_e
\end{aligned}
\qquad (6.25)
$$

Sometimes, however, the Q-value for a positron decay process is quoted as $Q = \Delta M$, and then a $2m_e c^2$ adjustment, namely 1·02 MeV, must be made in calculating the maximum *positron* energy. In each case, if the decay process leads to a state of excitation E_γ in the final nucleus, the Q-values are reduced by E_γ. The actual observable kinetic energy for a given Q is subject to a correction for c.m. motion, but this is very small for leptonic processes (see Ex. 10.3).

The width of the valley in the mass surface in which stable nuclei are found is determined by the criteria of β-stability (6.24). Other types of spontaneous decay such as α-particle emission may be energetically possible, but are often highly retarded by barrier effects. For $Z > 83$, however, the β-stable nuclei are actually α-active.

6.6 Nuclidic abundance (Ref. 6.5)

The abundance of the chemical *elements* in nature does not differ greatly, on present evidence, between the solar system and the rest

of the universe. The standard solar-system number abundance is conventionally related to the number of silicon atoms (Si $\equiv 10^6$) and is derived in large part from observations on meteorites, since terrestrial samples have been subject to chemical dispersion during geological time. For the stars and for interstellar space, spectroscopic and cosmic-ray observations are used. The interest in this data is its connection with the processes of element building through nuclear reactions that have taken place in stars. The end-products of this nucleosynthesis also contain information relevant to nuclear stability rules and to nuclear structure.

Such information is best sought in the abundance figures for specific *nuclides* (N, Z), which can be obtained from the elemental data using isotope ratios measured in both meteoritic and terrestrial samples. The main conclusions from both the elemental and nuclidic abundances are that:

(*a*) The elements of highest abundance in the universe are hydrogen and helium.
(*b*) There is a deficiency of the elements Li, Be and B in solar-system abundances presumably because the corresponding nuclides are readily consumed in nucleosynthesis. The cosmic rays, however, contain larger relative quantities of these nuclei, because they can be produced by interactions in interstellar space.
(*c*) Beyond the light elements a marked peak in the abundance of the even-Z, even-N nuclei occurs around $A = 56$ (Fig. 6.7) which correlates with the maximum binding energy shown for this A-value in Fig. 6.3. These are the most stable elements, and would be formed as end-products of an element-building stage in which thermal equilibrium was reached.
(*d*) Beyond the iron group, distinct peaks are seen at A-values corresponding with neutron numbers $N = 50$, 82 and 126. If these nuclides are built from lighter species by successive neutron capture and β^--decay then such peaks will be expected when a shell closes because the next neutron is less tightly bound (Ch. 7). Arguments can be given to relate the additional peaks at $A = 80$, 130 and 194 to the same shell structure.

Further evidence for shell structure in nuclei from abundance data comes from an examination of the distribution of *isotopes* (Z constant) and *isotones* (N constant) with respect to the line of stability shown by Fig. 2.1, p. 51. It is found that

(*e*) The number of stable and long-lived isotopes is greater for $Z = 20$, 28, 50 and 82 than for nearby elements.
(*f*) The number of stable and long-lived isotones is greater for $N = 20$, 28, 50, 82 and 126 than for nearby N-values.

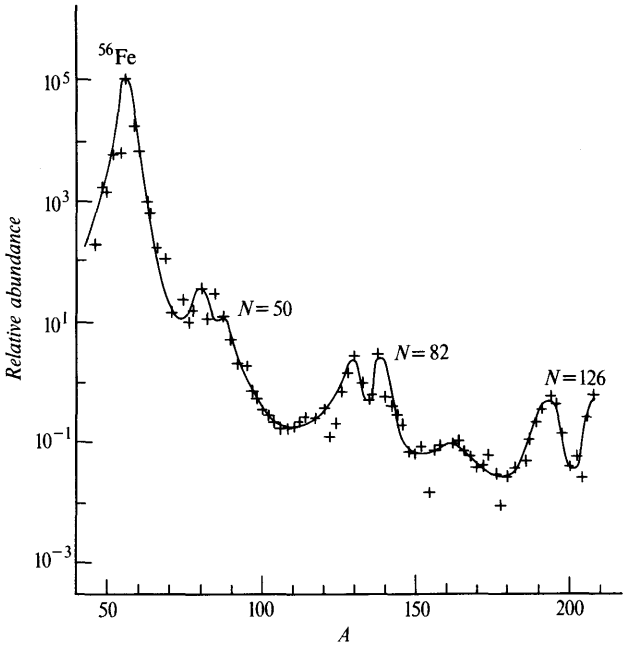

Fig. 6.7 Relative abundance (number of atoms) for even Z, even N nuclides as a function of mass number A for $A > 50$ (Ref. 6.2).

The distribution of stable nuclides according to individual neutron and proton numbers is given in Table 6.3 (taken from Ref. 2.1). The figures in the table illustrate the effect of the general properties of the nucleon–nucleon interaction, operating in nuclear matter. Thus, the approximate equality of number of odd-Z – even-N and odd-N – even-Z nuclides suggest the equivalence of neutrons and protons in element-building reactions (charge symmetry). The preponderance of even-Z – even-N nuclides is a direct consequence of the pairing force. The presence of two *unpaired* nucleons, as in nuclides of odd Z and odd N, results in instability in all but the lightest nuclei ^{2}H, ^{6}Li, ^{10}B and ^{14}N.

TABLE 6.3 Distribution of stable nuclides (Ref. 2.1)

A	Z	N	*Number of cases*
odd	odd	even	50
odd	even	odd	55
even	odd	odd	4
even	even	even	165

6.7 Summary

The most important 'bulk' properties of a nucleus are its mass and its size, to which all constituent nucleons contribute. Definitions are given of the atomic mass unit and of binding energy, separation energy and pairing energy. The binding energy is described by a semi-empirical formula and some understanding of the origin of its main attractive term has been reached by nuclear matter calculations. The particular role of pairing effects in the low-lying states of finite nuclei is emphasized.

Examples 6

6.1* Write down the total kinetic energy of a gas containing N neutrons and Z protons, regarding these as independent particles. By comparing this energy with that for the case $Z = N = A/2$, deduce the form of the asymmetry energy.

6.2* The scattering of α-particles through 60° by lead ($Z = 82$) begins to deviate appreciably from the predicted Coulomb value at an energy of 27 MeV. Estimate a radius for the target nuclei.

6.3 What is the mean-square radius of a square-well charge distribution of radius R? [$\frac{3}{5}R^2$]

6.4 The energy release in the reaction A(d, p)B is Q. Show that the neutron separation energy for nucleus B is $S_n = Q + \varepsilon$ where ε is the binding energy of the deuteron.

6.5* Calculate the level shift of the electron in a hydrogen atom due to the finite size of the nucleus, assuming a proton radius $R = 0{\cdot}6 \times 10^{-15}$ m. (Use first-order perturbation theory, and take the hydrogenic wavefunction to be $(1/\pi a_0^3)^{1/2} \exp(-r/a_0)$.)

6.6 Oxygen has isotopes of mass numbers 16, 17, 18 with relative abundance 99·758, 0·0373 and 0·2039. If Avogadro's number on the physical scale with $^{16}O = 16$ is $6{\cdot}0249 \times 10^{23}$ calculate its value on the chemical scale ($O = 16$). Find also the value of this constant on the physical scale with $^{12}C = 12$ if the mass of ^{12}C on the ^{16}O scale is 12·0039. [$6{\cdot}0233 \times 10^{23}$, $6{\cdot}0229 \times 10^{23}$]

6.7 Calculate the binding energy B, the binding energy per nucleon B/A, and the neutron and proton separation energies S_n, S_p for ^{114}Cd given that the mass excesses (i.e. the difference between the mass in a.m.u. and the mass number A) are p = 7·29 MeV, n = 8·07 MeV, ^{114}Cd = −90·01 MeV, ^{113}Cd = −89·04 MeV, ^{113}Ag = −87·04 MeV. [972·55, 8·53, 9·04, 10·26 MeV]
Compare your results with prediction from the semi-empirical mass formula with the constants given in the text.

6.8 Consider a large spherical nucleus of radius R containing A nucleons. At what total mass would the gravitational energy per nucleon equal a nuclear kinetic energy $\hbar^2/2m_p r_0^2$ with $r_0 = 1{\cdot}2$ fm? [$\approx 10^{29}$ kg]

6.9 Show that in a Fermi gas of neutrons the number of degenerate states with energy less than $\hbar^2 k^2/2m_n$ is $(2/9\pi)(kR)^3$ where R is the linear dimension of the containing volume.

6.10 No decay process linking the nuclei $^{150}_{60}$Nd and $^{150}_{61}$Pm is known. The (atomic) mass difference between the nuclei $^{150}_{60}$Nd and $^{150}_{62}$Sm has, however, been measured as 3633 ± 4 micromass units on the carbon scale and the accepted decay energy for the beta process $^{150}_{61}\text{Pm} \rightarrow {}^{150}_{62}\text{Sm}$ is 3·46 ± 0·03 MeV. Determine the relative stability of ^{150}Nd and ^{150}Pm and the decay energy. Suggest a possible mode of decay. [76 ± 30 keV, EC]

6.11 Given that the mass defect curve falls from +0·14 mass units for uranium to

−0·06 mass units in the middle of the periodic table, estimate in kWh the energy which could theoretically be obtained from 1 kg of ^{235}U. [$2{\cdot}7\times10^{7}$]

6.12 Assuming that the binding energy of an even-A nucleus may be written

$$-B(A,Z)=f(A)+\frac{0{\cdot}083}{A}(A/2-Z)^2+0{\cdot}000\,627Z^2/A^{1/3}\pm0{\cdot}036A^{-3/4}\text{ a.m.u.}$$

(+ for Z odd, − for Z even) determine the number of stable nuclides of mass $A=36$. Take $A^{1/3}=3{\cdot}3$, $A^{1/4}=2{\cdot}45$ and confine your attention to the range $13\leqslant Z\leqslant20$. [2]

6.13 In the carbon atom the K-edge is at 300 eV and the L_I-, L_{II}-edges at 60 eV. The atomic mass is 12·0000. Calculate:

(*a*) the mass of the carbon nucleus in a.m.u. neglecting electron binding [11·996 71]

(*b*) the percentage correction introduced when electron binding is allowed for. [10^{-5}]

6.14 The tabulated masses of $^{9}_{3}$Li, $^{9}_{4}$Be and $^{9}_{5}$B are 9·0268, 9·0122 and 9·0133 a.m.u. Calculate the value of the asymmetry coefficient in the semi-empirical mass formula, equation (6.10), ($M_H=1{\cdot}007\,83$, $M_n=1{\cdot}008\,67$ a.m.u.). [16 MeV]

6.15 From observation of the decay fragments of the hypernucleus ^{11}B it is found that the binding energy of the Λ-particle in this nucleus is 10·24 MeV. If the mass of ^{10}B is 10·0129 a.m.u., what is the mass of $^{11}_{\Lambda}$B? ($m_\Lambda=1115\text{ MeV}/c^2$). [11·1995 a.m.u.]

6.16 Estimate the energy of the μK X-ray for a phosphorus nucleus ($Z=15$), given that the ionization potential for hydrogen is 13·5 eV. [472 keV]

6.17 For any given muonic atom, calculate the principal quantum number of the muonic orbit that is just inside the electronic K-shell. [14]

6.18* For a uniform-density nucleus of (sharp) radius R show that the form factor for electron scattering with momentum transfer $q\hbar$ is, apart from a normalizing factor, $F(q)=[\sin qR-qR\cos qR]/q^3$. Compute the quantity $|F(q)|^2$ for points in the range $0{\cdot}1<qR<5{\cdot}0$.